

Electroweak Radiative Corrections to $\gamma\gamma \rightarrow W^+W^-$ †

A. DENNER

*Institut für Theoretische Physik, Universität Würzburg
Am Hubland, D-97074 Würzburg, Germany*

S. DITTMAYER

*Theoretische Physik, Universität Bielefeld
Postfach 100131, D-33501 Bielefeld, Germany*

R. SCHUSTER‡

*Institut für Theoretische Physik, Universität Würzburg
Am Hubland, D-97074 Würzburg, Germany***Abstract:**

We discuss the complete virtual and soft-photonic $\mathcal{O}(\alpha)$ corrections to $\gamma\gamma \rightarrow W^+W^-$ within the electroweak Standard Model for arbitrary polarized photons. In the on-shell renormalization scheme for fixed M_W no leading corrections associated with the running of α or heavy top-quark and Higgs-boson masses occur. The corrections turn out to be of the order of 10%, but can become much larger where the lowest-order cross-sections are suppressed.

BI-TP 96/03
WUE-ITP-96-001

January 1996

†Contribution to the Proceedings of the Workshop on *Physics with e^+e^- -Colliders*, Annecy, Genève, Hamburg, February 4 to September 1, 1995.

‡Supported by the Deutsche Forschungsgemeinschaft.

Electroweak Radiative Corrections to $\gamma\gamma \rightarrow W^+W^-$

A. Denner¹, S. Dittmaier² and R. Schuster^{1,†}

¹ *Institut für Theoretische Physik, Universität Würzburg, Germany*

² *Theoretische Physik, Universität Bielefeld, Germany*

1 Introduction

A particularly interesting process at $\gamma\gamma$ colliders is W-pair production. Its total cross-section approaches a constant of about 80 pb at high energies corresponding to 8×10^5 W pairs for 10 fb^{-1} . Although this large cross-section is drastically reduced by angular cuts, even for $|\cos\theta| < 0.8$ it is still 15 and 4 pb at a center-of-mass energy of 500 and 1000 GeV, respectively, and thus much larger as e.g. the one for $e^+e^- \rightarrow W^+W^-$. Hence $\gamma\gamma \rightarrow W^+W^-$ is very well-suited for precision investigations of the SM.

Most of the existing works on $\gamma\gamma \rightarrow W^+W^-$ concentrated on tree-level predictions and on the influence of anomalous non-Abelian gauge couplings [1, 2, 3]. At tree level, the process $\gamma\gamma \rightarrow W^+W^-$ depends both on the triple γWW and the quartic $\gamma\gamma WW$ coupling, and no other vertices are involved in the unitary gauge. The sensitivity to the γWW coupling is comparable and complementary to the reactions $e^+e^- \rightarrow W^+W^-$ and $e^-\gamma \rightarrow W^-\nu$ [2]. Because the sensitivity to the $\gamma\gamma WW$ coupling is much larger than the one in e^+e^- processes, $\gamma\gamma \rightarrow W^+W^-$ is the ideal process to study this coupling [3].

The one-loop diagrams involving a resonant Higgs boson have been calculated in order to study the possible investigation of the Higgs boson via $\gamma\gamma \rightarrow H^* \rightarrow W^+W^-$ [4, 5, 6, 7]. Based on our complete one-loop calculation [8], we have supplemented these investigations by a discussion of the heavy-Higgs effects in Ref. [9]. As a matter of fact, only the (suppressed) channels of longitudinal W-boson production are sensitive to the Higgs mechanism, but the (dominant) channels of purely transverse W-boson production are extremely insensitive. This insensitivity to the Higgs sector renders $\gamma\gamma \rightarrow W^+W^-$ even more suitable for the investigation of the non-Abelian self couplings.

In this paper we summarize our results for the *complete* virtual and soft-photonic $\mathcal{O}(\alpha)$ corrections. We give a survey of the leading corrections and restrict the numerical

[†]Supported by the Deutsche Forschungsgemeinschaft.

discussion to unpolarized W bosons. More detailed results and a discussion of their evaluation can be found in Refs. [8, 9].

2 Lowest-order cross-section

The Born cross-section of $\gamma\gamma \rightarrow W^+W^-$ is given by the formulae

$$\left(\frac{d\sigma}{d\Omega}\right)_{\text{unpol}}^{\text{Born}} = \frac{3\alpha^2\beta}{2s} \left\{ 1 - \frac{2s(2s + 3M_W^2)}{3(M_W^2 - t)(M_W^2 - u)} + \frac{2s^2(s^2 + 3M_W^4)}{3(M_W^2 - t)^2(M_W^2 - u)^2} \right\} \quad (1)$$

for the unpolarized differential cross-section and

$$\sigma_{\text{unpol}}^{\text{Born}} = \frac{6\pi\alpha^2}{s} \beta \cos \theta_{\text{cut}} \left\{ 1 - \frac{4M_W^2(s - 2M_W^2)}{s^2\beta \cos \theta_{\text{cut}}} \log \left(\frac{1 + \beta \cos \theta_{\text{cut}}}{1 - \beta \cos \theta_{\text{cut}}} \right) + \frac{16(s^2 + 3M_W^4)}{3s^2(1 - \beta^2 \cos^2 \theta_{\text{cut}})} \right\} \quad (2)$$

for the unpolarized cross-section integrated over $\theta_{\text{cut}} < \theta < 180^\circ - \theta_{\text{cut}}$. Here $\beta = \sqrt{1 - 4M_W^2/s}$ denotes the velocity of the W bosons and s , t , and u are the usual Mandelstam variables. Concerning kinematics, polarizations, input parameters, etc., we follow the conventions of Ref. [8] throughout.

As can be seen from Table 1, the lowest-order cross-sections are dominated by transverse (T) W bosons. The massive t -channel exchange gives rise to a constant cross-section at high energies, $s \gg M_W^2$, for $\theta_{\text{cut}} = 0$

$$\sigma_{\pm\pm\text{UU}}^{\text{Born}}, \sigma_{\pm\mp\text{UU}}^{\text{Born}} \xrightarrow{s \rightarrow \infty} \sigma_{\pm\pm\text{TT}}^{\text{Born}}, \sigma_{\pm\mp\text{TT}}^{\text{Born}} \xrightarrow{s \rightarrow \infty} \frac{8\pi\alpha^2}{M_W^2} = 80.8 \text{ pb.} \quad (3)$$

For a finite cut, $\sigma_{\pm\pm\text{UU}}^{\text{Born}}$ and $\sigma_{\pm\mp\text{UU}}^{\text{Born}}$ behave as $1/s$ for large s . This is illustrated in Fig. 1 for two different angular cuts $\theta_{\text{cut}} = 10^\circ, 20^\circ$. Close to threshold the differential and integrated cross-sections for all polarization configurations vanish like β .

3 Leading corrections

Electroweak radiative corrections contain leading contributions of universal origin. In the on-shell renormalization scheme with input parameters α , M_W , M_Z these affect the corrections to $\gamma\gamma \rightarrow W^+W^-$ as follows:

- Since the *two* external photons are on mass shell, the relevant effective coupling is the one at zero-momentum transfer and the running of α is not relevant.

\sqrt{s}/GeV	θ	unpol	$\pm\pm\text{TT}$	$\pm\pm\text{LL}$	$\pm\mp\text{TT}$	$\pm\mp\text{LL}$	$\pm\mp(\text{LT} + \text{TL})$
500	$0^\circ < \theta < 180^\circ$	77.6	82.2	6.10×10^{-2}	70.2	9.99×10^{-1}	1.69
	$20^\circ < \theta < 160^\circ$	36.7	42.7	3.17×10^{-2}	28.2	9.89×10^{-1}	1.49
1000	$0^\circ < \theta < 180^\circ$	80.1	82.8	3.54×10^{-3}	76.9	2.52×10^{-1}	1.70×10^{-1}
	$20^\circ < \theta < 160^\circ$	14.2	16.8	7.18×10^{-4}	11.2	2.44×10^{-1}	1.21×10^{-1}
2000	$0^\circ < \theta < 180^\circ$	80.6	81.6	2.14×10^{-4}	79.5	6.41×10^{-2}	1.50×10^{-2}
	$20^\circ < \theta < 160^\circ$	4.07	4.84	1.27×10^{-5}	3.23	6.11×10^{-2}	8.26×10^{-3}

Table 1: *Lowest-order integrated cross-sections in pb for several polarizations; the lowest-order cross-section for $\pm\pm(\text{LT} + \text{TL})$ vanishes.*

- In order to handle the Higgs-boson resonance at $s = M_{\text{H}}^2$, in the literature [5, 6, 7] the Higgs-boson width has been introduced naïvely by the replacement

$$\frac{F^H(s)}{s - M_{\text{H}}^2} \longrightarrow \frac{F^H(s)}{s - M_{\text{H}}^2 + iM_{\text{H}}\Gamma_{\text{H}}} \quad (4)$$

in the resonant contribution. However, this treatment destroys gauge invariance at the level of non-resonant $\mathcal{O}(\alpha)$ corrections. In order to preserve gauge invariance, we decompose the Higgs-resonance contribution into a gauge-invariant resonant part and a gauge-dependent non-resonant part and introduce Γ_{H} only in the former:

$$\frac{F^H(s)}{s - M_{\text{H}}^2} \longrightarrow \frac{F^H(M_{\text{H}}^2)}{s - M_{\text{H}}^2 + iM_{\text{H}}\Gamma_{\text{H}}} + \frac{F^H(s) - F^H(M_{\text{H}}^2)}{s - M_{\text{H}}^2}. \quad (5)$$

- Outside the region of Higgs resonance the Higgs-mass dependence is small for unpolarized W bosons. For all polarizations no corrections involving $\log(M_{\text{H}}/M_{\text{W}})$ or $M_{\text{H}}^2/M_{\text{W}}^2$ arise in the heavy-Higgs limit [9]. However, for $\sqrt{s} \gg M_{\text{H}} \gg M_{\text{W}}$ corrections proportional to $M_{\text{H}}^2/M_{\text{W}}^2$ appear for the cross-sections involving longitudinal (L) gauge bosons as a remnant of the unitarity cancellations. These terms give rise to large effects in particular for cross-sections with longitudinal W bosons.
- The top-mass-dependent corrections are also small and behave similar to the Higgs-mass-dependent corrections for $\sqrt{s} \gg m_{\text{t}} \gg M_{\text{W}}$; more precisely neither corrections proportional to m_{t}^2 nor proportional to $\log m_{\text{t}}$ occur in this limit for fixed M_{W} .
- As $\gamma\gamma \rightarrow \text{W}^+\text{W}^-$ involves no light charged external particles, no large logarithmic corrections associated with collinear photons show up (apart from the region of very high energies, $s \gg M_{\text{W}}^2$). As a consequence, the photonic corrections are not enhanced with respect to the weak corrections.

- Close to threshold, i.e. for $\beta \ll 1$, the Coulomb singularity gives rise to the large universal correction

$$\delta\sigma^{\text{Coul.}} = \frac{\alpha\pi}{2\beta}\sigma^{\text{Born}}. \quad (6)$$

The factor β^{-1} is typical for the pair production of stable (on-shell) particles. For the generalization to unstable (off-shell) particles see Ref. [10].

At high energies, $s \gg M_W^2$, the radiative corrections are dominated by terms like $(\alpha/\pi)\log^2(s/M_W^2)$, which arise from vertex and box diagrams. At 1 TeV these are about 10%, setting the scale for the (weak) radiative corrections at this energy.

4 Numerical results

Electromagnetic and genuine weak corrections cannot be separated in a gauge-invariant way on the basis of Feynman diagrams. As no leading collinear logarithms occur in $\gamma\gamma \rightarrow W^+W^-$, the only source of enhanced photonic corrections are the soft-photon-cut-off-dependent terms which yield the relative correction

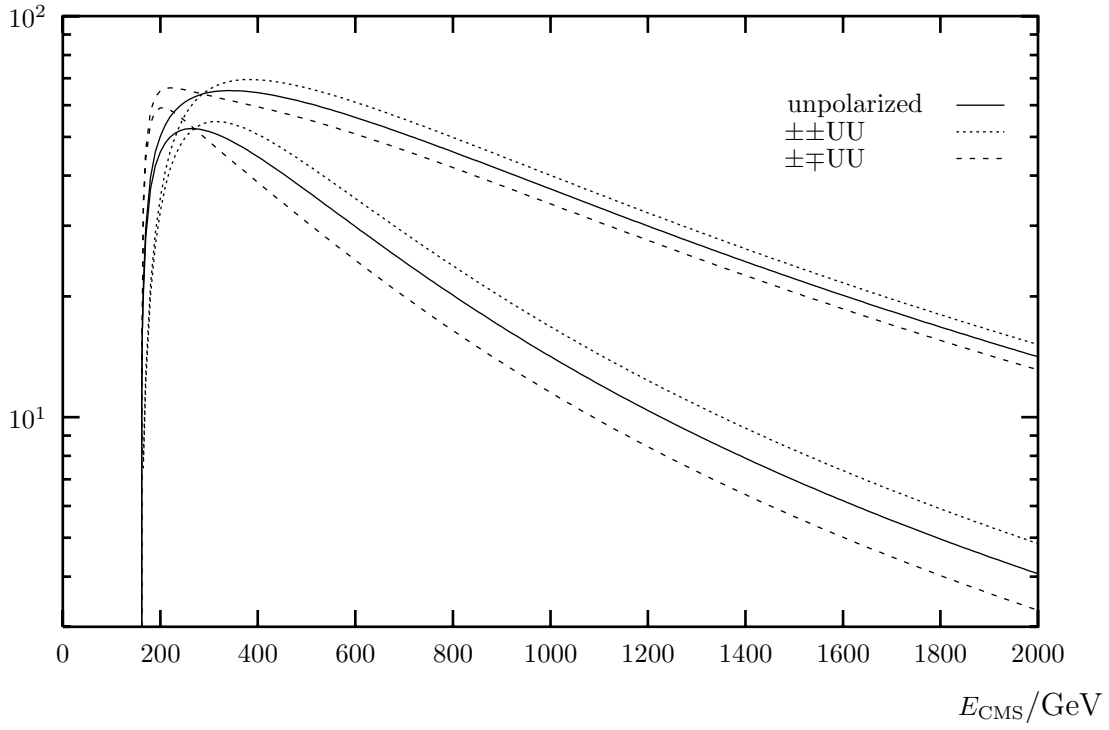
$$\delta_{\text{cut}} = -\frac{2\alpha}{\pi} \log\left(\frac{\Delta E}{E}\right) \left(1 - \frac{s - 2M_W^2}{s\beta} \log\frac{1 + \beta}{1 - \beta}\right). \quad (7)$$

Since we are mainly interested in the weak corrections, we discard the (gauge-invariant) cut-off-dependent terms (7) by setting the soft-photon cut-off energy ΔE equal to the beam energy E and consider the rest as a suitable measure of the weak corrections. If not stated otherwise, the correction δ stands in the following for the complete relative soft-photonic and virtual electroweak corrections with $\Delta E = E$.

Figure 1 shows the “weak” corrections to the total cross-sections integrated over $10^\circ \leq \theta \leq 170^\circ$ and $20^\circ \leq \theta \leq 160^\circ$ for unpolarized W bosons. The corrections for different photon polarizations almost coincide with each other and reach roughly -20% for $\theta_{\text{cut}} = 10^\circ$ and -35% for $\theta_{\text{cut}} = 20^\circ$ at $\sqrt{s} = 2$ TeV. At low energies the cross-sections with equal photon and W boson helicities are dominated by the Higgs resonance. Note that owing to helicity conservation the other cross-sections are not affected by the Higgs resonance.

In Table 2 we list the unpolarized cross-sections and the corresponding corrections for several energies and scattering angles. We include the corrections for a soft-photon-energy cut-off $\Delta E = 0.1E$, i.e. the cut-off-dependent corrections δ_{cut} from (7), and the individual (gauge-invariant) fermionic δ_{ferm} and bosonic corrections δ_{bos} . The fermionic corrections consist of all loop diagrams and counterterm contributions involving fermion loops, all

$\sigma^{\text{Born}}/\text{pb}$



$\delta/\%$

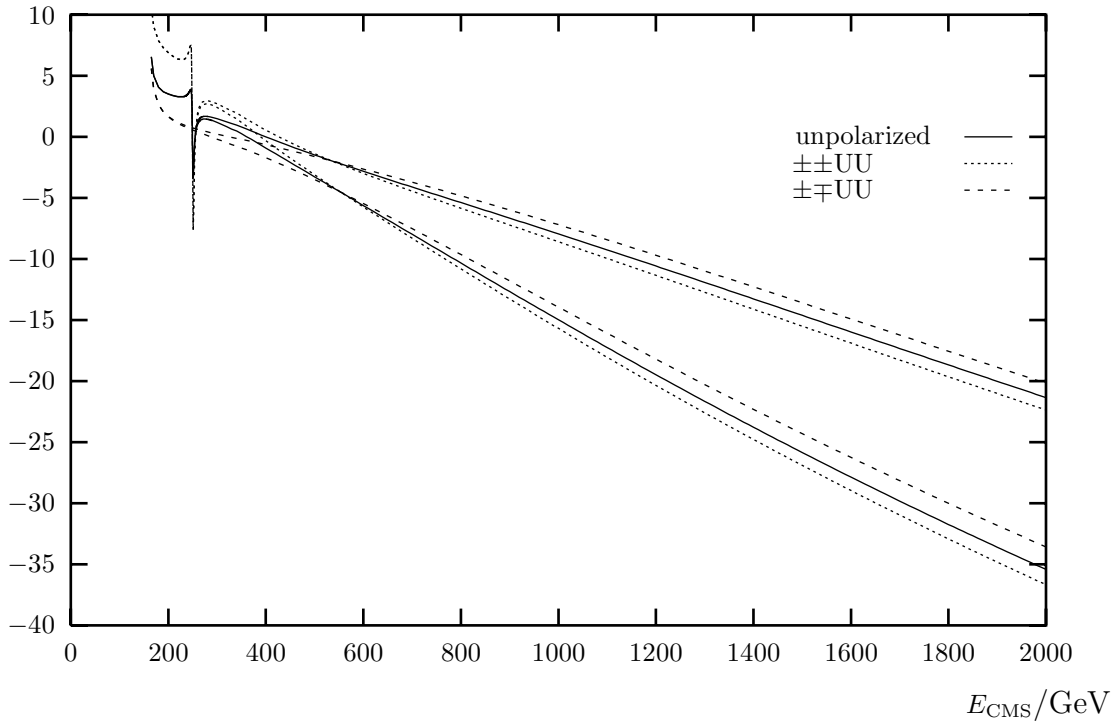


Figure 1: *Integrated lowest-order cross-sections and corresponding relative corrections for an angular cut $10^\circ \leq \theta \leq 170^\circ$ (upper set of curves in each plot) and $20^\circ \leq \theta \leq 160^\circ$ (lower set).*

\sqrt{s}/GeV	θ	$\sigma^{\text{Born}}/\text{pb}$	$\delta_{\Delta E=0.1E}/\%$	$\delta_{\text{cut}}/\%$	$\delta_{\Delta E=E}/\%$	$\delta_{\text{bos}}/\%$	$\delta_{\text{ferm}}/\%$
500	5°	98.13	0.02	-2.79	2.81	1.49	1.32
	20°	26.04	-2.68	-2.79	0.11	-0.08	0.19
	90°	0.724	-10.79	-2.79	-8.00	-5.62	-2.38
	$0^\circ < \theta < 180^\circ$	77.55	-3.38	-2.79	-0.59	-0.65	0.06
	$10^\circ < \theta < 170^\circ$	60.74	-4.27	-2.79	-1.48	-1.21	-0.27
	$20^\circ < \theta < 160^\circ$	36.67	-6.06	-2.79	-3.27	-2.39	-0.89
1000	5°	291.9	-2.06	-4.31	2.25	1.04	1.21
	20°	15.61	-11.90	-4.31	-7.59	-6.37	-1.22
	90°	0.193	-31.64	-4.31	-27.33	-21.93	-5.40
	$0^\circ < \theta < 180^\circ$	80.05	-7.08	-4.31	-2.77	-2.71	-0.06
	$10^\circ < \theta < 170^\circ$	37.06	-12.26	-4.31	-7.95	-6.65	-1.30
	$20^\circ < \theta < 160^\circ$	14.16	-19.29	-4.31	-14.98	-12.20	-2.78
2000	5°	418.8	-7.14	-5.80	-1.33	-1.59	0.25
	20°	5.163	-30.31	-5.80	-24.51	-20.96	-3.55
	90°	0.049	-59.59	-5.80	-53.78	-45.47	-8.32
	$0^\circ < \theta < 180^\circ$	80.59	-9.85	-5.80	-4.04	-3.95	-0.09
	$10^\circ < \theta < 170^\circ$	14.14	-27.15	-5.80	-21.35	-18.34	-3.01
	$20^\circ < \theta < 160^\circ$	4.068	-41.22	-5.80	-35.41	-30.12	-5.29

Table 2: *Lowest-order cross-sections and relative corrections for unpolarized particles*

other contributions form the bosonic corrections. The fermionic corrections stay below 5–10% even for high energies. The bosonic contributions are responsible for the large corrections at high energies, in particular in the central angular region.

In Ref. [2] the total cross-section and the ratios

$$R_{10} = \frac{\sigma(|\cos \theta| < 0.4)}{\sigma(|\cos \theta| < 0.8)}, \quad R_{\text{LT}} = \frac{\sigma_{\text{LL}}}{\sigma_{\text{TT}}}, \quad R_{02} = \frac{\sigma_{++}}{\sigma_{+-}}. \quad (8)$$

have been investigated in view of their sensitivity to anomalous couplings.¹ We list the lowest-order predictions together with the $\mathcal{O}(\alpha)$ -corrected ones and the relative “weak” corrections for these observables in Table 3 using $|\cos \theta_{\text{cut}}| = 0.8$.

In Fig. 2 we plot the integrated cross-section including $\mathcal{O}(\alpha)$ “weak” corrections using $\theta_{\text{cut}} = 20^\circ$ for various values of the Higgs-boson mass. While the Higgs resonance is comparably sharp for small Higgs-boson masses, it is washed out by the large width of the Higgs boson for high M_{H} . Already for $M_{\text{H}} = 400 \text{ GeV}$ the Higgs resonance is hardly visible.

¹Note that we do not perform a convolution with a realistic photon spectrum but consider the incoming photons as monochromatic.

\sqrt{s}/GeV		σ/pb	R_{IO}	R_{LT}	R_{02}
500	Born level	15.74	0.265	0.0308	1.934
	corrected	14.82	0.259	0.0325	1.950
	corrections/%	-5.83	-2.02	5.43	0.78
1000	Born level	4.659	0.241	0.0235	2.229
	corrected	3.617	0.227	0.0276	2.184
	corrections/%	-22.36	-5.64	17.08	-2.05
2000	Born level	1.218	0.234	0.0220	2.307
	corrected	0.647	0.207	0.0321	2.168
	corrections/%	-46.86	-11.53	46.11	-6.02

Table 3: *Tree-level and $\mathcal{O}(\alpha)$ results for various observables using $|\cos\theta_{\text{cut}}| = 0.8$*

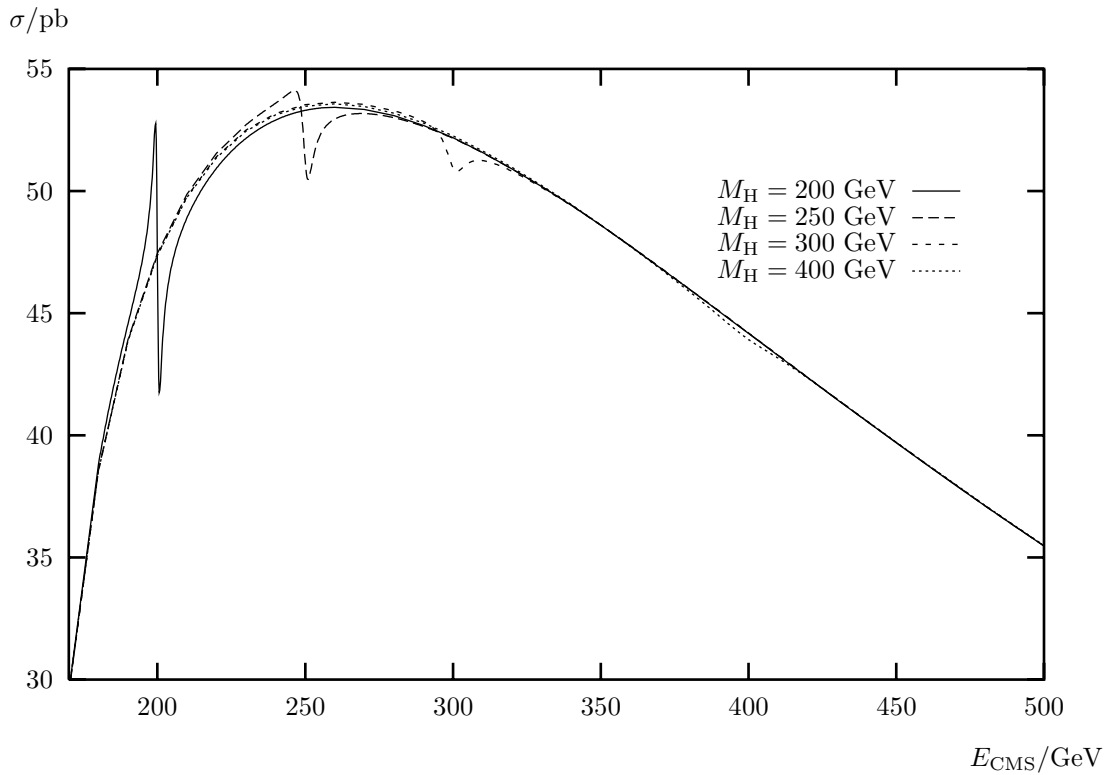


Figure 2: *Integrated unpolarized cross-section including $\mathcal{O}(\alpha)$ “weak” corrections for various Higgs-boson masses ($20^\circ < \theta < 160^\circ$)*

5 Summary

The process $\gamma\gamma \rightarrow W^+W^-$ will be one of the most interesting reactions at future $\gamma\gamma$ colliders. In particular, it is very useful to study non-Abelian gauge couplings.

We have calculated the one-loop radiative corrections to $\gamma\gamma \rightarrow W^+W^-$ within the electroweak Standard Model in the soft-photon approximation for arbitrary polarizations of the photons and W bosons. An interesting peculiarity of $\gamma\gamma \rightarrow W^+W^-$ is the absence of most universal leading corrections, such as the running of α and leading logarithms associated with collinear bremsstrahlung. Therefore, theoretical predictions are very clean. The variation of the cross-sections with the top-quark and Higgs-boson masses is small if M_W is kept fixed with the exception of the cross-sections involving longitudinal W bosons at high energies. In the heavy mass limit no leading m_t^2 -, $\log m_t$ -, and $\log M_H$ -terms exist.

The soft-photon-cut-off-independent radiative corrections to the total cross-section are of the order of 10% and can reach up to 50% at 2 TeV. The large corrections are due to bosonic loop diagrams whereas the effects of the fermionic ones are of the order of 5–10%.

References

- [1] K.J. Kim and Y.S. Tsai, *Phys. Rev.* **D8** (1973) 3109;
G. Tupper and M.A. Samuel, *Phys. Rev.* **D23** (1981) 1933;
S.Y. Choi and F. Schrempp, *Phys. Lett.* **B272** (1991) 149.
- [2] E. Yehudai, *Phys. Rev.* **D44** (1991) 3434.
- [3] G. Bélanger and F. Boudjema, *Phys. Lett.* **B288** (1992) 210.
- [4] M.A. Shifman et al., *Sov. J. Nucl. Phys.* **30** (1979) 711.
- [5] E.E. Boos and G.V. Jikia, *Phys. Lett.* **B275** (1992) 164.
- [6] D.A. Morris, T.N. Truong and D. Zappalá, *Phys. Lett.* **B323** (1994) 421.
- [7] H. Veltman, *Z. Phys.* **C62** (1994) 235.
- [8] A. Denner, S. Dittmaier and R. Schuster, *Nucl. Phys.* **452** (1995) 80.
- [9] A. Denner, S. Dittmaier and R. Schuster, *Phys. Rev.* **D51** (1995) 4738.
- [10] V.S. Fadin, V.A. Khoze and A.D. Martin, *Phys. Lett.* **B311** (1993) 311; *Phys. Rev.* **D52** (1995) 1377;
D. Bardin, W. Beenakker and A. Denner, *Phys. Lett.* **B317** (1994) 213.